

This is the accepted manuscript made available via CHORUS. The article has been published as:

Revealing the pseudogap in
 $\text{Sr}_{\{3\}}(\text{Ru}_{\{0.985\}}\text{Fe}_{\{0.015\}})_{\{2\}}\text{O}_{\{7\}}$ by optical
spectroscopy

W. J. Ban, B. Xu, W. H. Li, Y. Wang, J. J. Ge, P. G. Li, R. Yang, Y. M. Dai, Z. Q. Mao, and H.
Xiao

Phys. Rev. B **98**, 205111 — Published 6 November 2018

DOI: [10.1103/PhysRevB.98.205111](https://doi.org/10.1103/PhysRevB.98.205111)

Revealing pseudogap in $\text{Sr}_3(\text{Ru}_{0.985}\text{Fe}_{0.015})_2\text{O}_7$ by optical spectroscopy study

W. J. Ban,¹ B. Xu,² W. H. Li,³ Y. Wang,⁴ J. J. Ge,⁴ P. G. Li,⁴ R. Yang,³ Y. M. Dai,⁵ Z. Q. Mao,⁴ and H. Xiao^{1,*}

¹Center for High Pressure Science and Technology Advanced Research, Beijing 100094, China

²University of Fribourg, Department of Physics and Fribourg Center for Nanomaterials, Chemin du Musée 3, CH-1700 Fribourg, Switzerland

³Institute of Physics, Chinese Academy of Sciences, Beijing, 100190 China

⁴Department of Physics and Engineering Physics, Tulane University, New Orleans, Louisiana, 70118, USA

⁵Center for Superconducting Physics and Materials, National Laboratory of Solid State

Microstructures and Department of Physics, Nanjing University, Nanjing 210093, China

We report resistivity, magnetization and optical spectroscopy study on single crystal sample $\text{Sr}_3(\text{Ru}_{0.985}\text{Fe}_{0.015})_2\text{O}_7$. An upturn is observed in resistivity at about 30 K. Below 30 K, the dip in resistivity $R(\omega)$, the suppression in scattering rate $1/\tau(\omega)$, the peak-like feature in optical conductivity $\sigma_1(\omega)$ and the remainder of spectral weight all suggest the formation of a pseudogap. What's more, one phonon peak at about 600 cm^{-1} is distinguished at all temperatures, which has asymmetric line shape. Such asymmetric line shape can be fit by a Fano function, the resulted Fano factor $1/q^2$ and linewidth γ show significant increasing below 30 K, giving further evidence for the formation of a pseudogap, which might originate from the partial k-space gap opening due to density wave instability.

INTRODUCTION

The Ruddlesden-Popper type $(\text{Ba,Sr,Ca})_{n+1}\text{Ru}_n\text{O}_{3n+1}$ ($n = 0, 1, 2, \dots, \infty$) have attracted significant attention due to the existence of rich electronic and magnetic phenomena in these materials, such as superconductivity, complex magnetism, metal-insulator transition (MIT), density wave (DW), quantum criticality and heavy fermions as well as pseudogap (PG) [1–22]. PG phenomena have been intensively investigated in high- T_C superconductors (HTSC) due to their possible connection to the superconducting mechanism [23–28]. PG phenomena have also been widely observed and investigated in $(\text{Ba,Sr,Ca})_{n+1}\text{Ru}_n\text{O}_{3n+1}$ ($n = 0, 1, 2, \dots, \infty$) series compounds. For example, the early optical spectroscopy study of Sr_2RuO_4 exhibited a gap-like behavior with a gap energy of 6.3 meV [22]. It could be coupled to gapped magnetic excitations, remind us of the PG behavior in HTSC. The optical conductivity spectra of four-layer and nine-layer BaRuO_3 compounds clearly displayed the formation of a PG [20, 21], however, four-layer BaRuO_3 shows a metallic Fermi-liquid-like behavior, while nine-layer BaRuO_3 has an insulator-like state at low temperature.

A quite interesting observation is that PG have also been widely observed in some strongly correlated materials near their resistivity-upturn temperature. Such as, the optical spectroscopy study of $\text{Ca}_3\text{Ru}_2\text{O}_7$ shows a PG opening around 200 cm^{-1} below 50 K, accompanied with an upturn of the resistivity at 48 K, which might be attributed to the partial gap opening due to the DW instability [29]. For $\text{Sr}_3\text{Ru}_2\text{O}_7$, with Ru site doping by a few percent of Mn, optical spectroscopy study shows the opening of a gap accompanied by the resistivity-upturn behavior [18], however, as the lack of datas below 600 cm^{-1} , they could not address whether there has a Drude-like peak as the compound enters the ground state below its resistivity-upturn temperature. So the optical data is not suffi-

cient enough to discuss whether there is a full gap or pseudogap opening phenomenon [30].

$\text{Sr}_3\text{Ru}_2\text{O}_7$ is a paramagnetic metal, and a system with strong magnetic fluctuations [11, 12, 31–33]. So the introduction of a magnetic field and magnetic doping can induce very interesting effects on the magnetic and electronic properties. The magnetic neutron scattering study of $\text{Sr}_3\text{Ru}_2\text{O}_7$ shows that the application of a magnetic field can tune it through two magnetically ordered spin density wave (SDW) states. Mn doped $\text{Sr}_3\text{Ru}_2\text{O}_7$ exhibits a commensurate E-type AFM order, accompanied by a resistivity-upturn behavior [18, 19, 34, 35]. However, $\text{Sr}_3(\text{Ru}_{1-x}\text{Fe}_x)_2\text{O}_7$ with Fe substitution for Ru, shows a metallic spin-glass-like state for $x = 0.01$, whereas an insulating-like, E-type AFM ordered phase is induced below $T_N \approx 40\text{ K}$ for $x \geq 0.03$, respectively [15].

With the purpose to know whether the PG opening phenomenon also exist in Fe doped $\text{Sr}_3\text{Ru}_2\text{O}_7$ and to reveal more information about the resistivity-upturn behavior, we perform resistivity and optical spectroscopy study on single crystal sample $\text{Sr}_3(\text{Ru}_{0.985}\text{Fe}_{0.015})_2\text{O}_7$. The resistivity shows a clear upturn at about 30 K. Below 30 K, a clear dip in resistivity $R(\omega)$ and a peak-like feature in optical conductivity $\sigma_1(\omega)$ were observed in far infrared range, accompanied by the suppression in scattering rate $1/\tau(\omega)$ and the remainder of spectral weight (SW), suggesting the formation of a PG. What's more, a phonon peak at about 600 cm^{-1} has asymmetric line shape, which can be fit by a Fano function, the resulted Fano factor $1/q^2$ and linewidth γ show significant increasing accompanied by the resistivity-upturn behavior, giving further evidence for the formation of a PG.

EXPERIMENTAL DETAILS

High quality $\text{Sr}_3(\text{Ru}_{1-x}\text{Fe}_x)_2\text{O}_7$ single crystals were grown using the floating zone technique [15]. The resulting crystals have dimensions of several millimeters. The actual Fe level was determined to be 0.015 by energy dispersive X-ray

(EDX) measurements on the as-grown single crystals. The dc resistivity was measured by a four-probe method, and the electrical current flows along the direction parallel to the ab plane of the crystal. The measurement was conducted on a commercial Quantum Design Physical Properties Measurement System (PPMS). The magnetic susceptibility was measured on a Quantum Design superconducting quantum interference device vibrating sample magnetometer system (SQUID-VSM). The optical reflectance measurements were performed on as-grown shiny surface of the single crystal with a Fourier transform infrared spectrometer (Bruker 80v) in the frequency range from 40 to 20000 cm^{-1} . An in-situ gold and aluminum over-coating technique was used to get the reflectance [36]. The measured reflectance was then corrected by multiplying the available curves of gold and aluminum reflectivity at different temperatures. The real part of conductivity $\sigma_1(\omega)$ was obtained by the Kramers-Kronig transformation of $R(\omega)$. The Hagen-Rubens relation was used for low-frequency extrapolation; on the high-frequency side, we employed an extrapolation method with X-ray atomic scattering functions [37]. This new extrapolation method is proved to be more effective and unambiguous in deriving and analyzing the optical constants.

RESULTS AND DISCUSSIONS

Figure 1 presents the temperature dependence of resistivity for $\text{Sr}_3(\text{Ru}_{0.985}\text{Fe}_{0.015})_2\text{O}_7$ single crystal. Upon cooling, the resistivity decreases continuously until 30 K. Below this temperature, the resistivity shows a clear upturn. Similar behaviors have been observed in Fe/Ti/Mn doped $\text{Sr}_3\text{Ru}_2\text{O}_7$ [15, 17, 18] and $\text{Ca}_3\text{Ru}_2\text{O}_7$ [29].

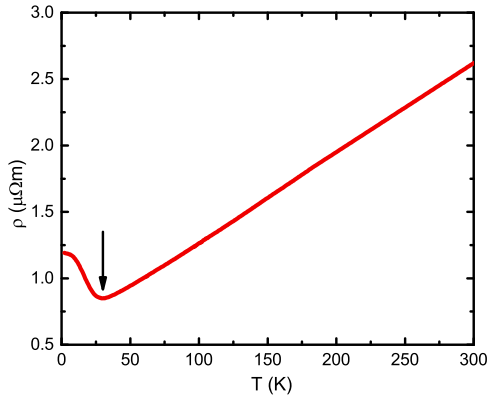


FIG. 1. The temperature dependent resistivity ρ of $\text{Sr}_3(\text{Ru}_{0.985}\text{Fe}_{0.015})_2\text{O}_7$. The black arrow denotes the resistivity-upturn temperature.

Figure 2 shows the temperature dependence of the magnetic susceptibility χ of $\text{Sr}_3(\text{Ru}_{0.985}\text{Fe}_{0.015})_2\text{O}_7$ under zero-field-cooled (ZFC) and field-cooled (FC) conditions, respectively. A sharp peak develops in magnetic suscep-

tibility χ_{ab} at about 30 K, suggestive of an onset of paramagnetic-antiferromagnetic phase transition. However, χ_c shows a bifurcation between the ZFC and FC data below about 22 K, characteristic of a spin-glass-like state, similar to $\text{Sr}_3(\text{Ru}_{0.985}\text{Fe}_{0.015})_2\text{O}_7$, which shows a paramagnetic-antiferromagnetic phase transition at about 10 K and enters a spin-glass-like state at 4 K [15].

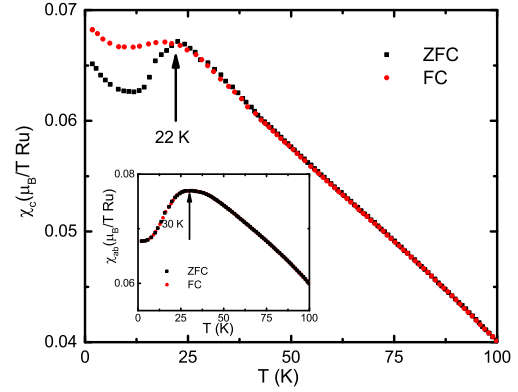


FIG. 2. The temperature dependent magnetic susceptibility χ_c of $\text{Sr}_3(\text{Ru}_{0.985}\text{Fe}_{0.015})_2\text{O}_7$ measured under zero-field-cooled (ZFC) and field-cooled (FC) conditions. Inset: χ_{ab} vs. T under ZFC and FC.

Figure 3(a) shows the reflectance spectra $R(\omega)$ of $\text{Sr}_3(\text{Ru}_{0.985}\text{Fe}_{0.015})_2\text{O}_7$ from 0 to 1500 cm^{-1} at several temperatures 35, 50, 100, 200 and 300 K, which are above the resistivity-upturn temperature. The high value of $R(\omega)$ which increases upon cooling reflects the metallic nature of this material.

However, below the resistivity-upturn temperature, the low frequency $R(\omega)$ decreases upon cooling (Fig. 3(b)), consistent with the upturn of the resistivity. And $R(\omega)$ becomes strongly suppressed in the region between 0 to 6500 cm^{-1} (inset of Fig. 3(a)); while a clear dip-like feature (as indicated by the black arrow in Fig. 3(b)) gradually developed at about 270 cm^{-1} and the lower ω reflectance increases faster than those of higher temperatures, which is a gap-like feature manifested in reflectance spectra. Besides, one phonon mode at about 600 cm^{-1} emerges in $R(\omega)$ at all temperatures, as indicated by the red arrow.

More insight into the evolution of the electronic states across the resistivity-upturn temperature is clearly reflected in the optical conductivity spectra. Fig. 4(a) illustrates the real part of optical conductivity $\sigma_1(\omega)$ at several temperatures below 50 K. The most prominent behavior in $\sigma_1(\omega)$ is that, below the resistivity-upturn temperature, the SW below about 200 cm^{-1} becomes gradually suppressed, the suppressed SW partially transfer to a peak-like feature with its central frequency at about 350 cm^{-1} (shown as the blue circle in Fig. 4(a)), which is a gap-like feature manifested in conductivity spectra [29]. It is interesting to note that as frequency decreases below about 180 cm^{-1} , $\sigma_1(\omega)$ increases and a very

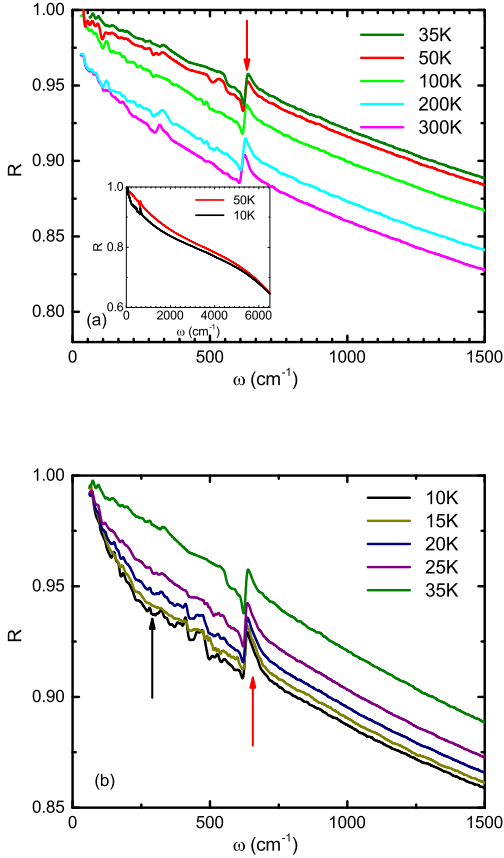


FIG. 3. (a) The reflectance spectra $R(\omega)$ of $\text{Sr}_3(\text{Ru}_{0.985}\text{Fe}_{0.015})_2\text{O}_7$ from 0 to 1500 cm^{-1} at several temperatures above 35 K. (b) The reflectance spectra $R(\omega)$ of $\text{Sr}_3(\text{Ru}_{0.985}\text{Fe}_{0.015})_2\text{O}_7$ from 0 to 1500 cm^{-1} at several temperatures below 35 K. The inset in (a) show the reflectivity of 10 and 50 K up to 6500 cm^{-1} . The black arrow denotes the dip-like feature in reflectance spectra. The red arrows denote the phonons.

148 narrow Drude-type component appears, this feature is differ-
 149 ent from the formation of an ordinary band gap insulating (or
 150 a semiconducting) state, where the SW in the gap-like region
 151 should disappear completely. The remainder of the SW below
 152 the resistivity-upturn temperature indicates that a PG is
 153 formed in this material.

154 To investigate the SW transfer more clearly, we have cal-
 155 culated the integrated SW between different lower and upper
 156 cutoff frequencies, which was defined as $W_S = \int_a^b \sigma_1(\omega)d\omega$.
 157 Fig. 5(a) illustrates the upper cut off frequency dependent
 158 SW at several representative temperatures. The ratio of W_S
 159 at low to high temperature $W_S(T_L)/W_S(T_H)$ is shown in Fig.
 160 5(b). $W_S(50\text{ K})/W_S(300\text{ K})$ exceeds 1 at low energy and then
 161 smoothly approach 1, indicates a transfer of SW from high-
 162 to low- energy region with decreasing temperature. The W_S
 163 transfer across the resistivity-upturn temperature can be more
 164 clearly seen in the plot of the ratio of the integrated SW at

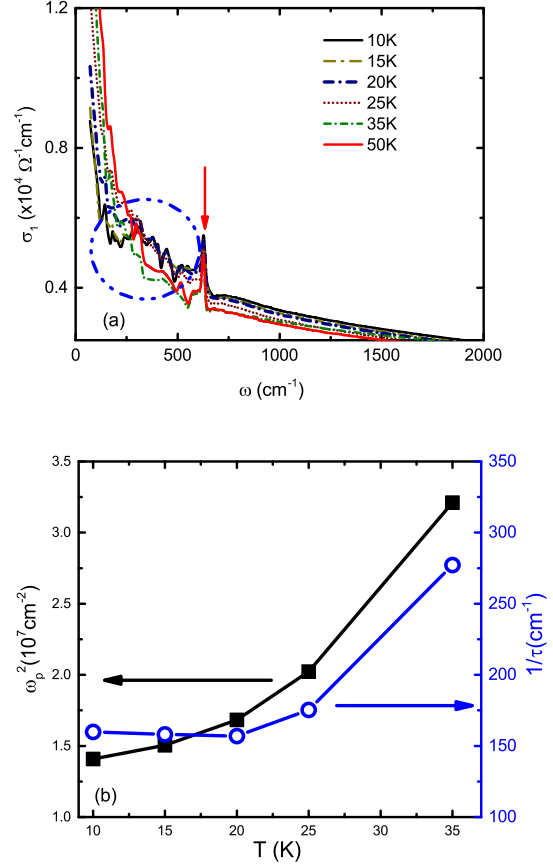


FIG. 4. (a) The temperature dependent optical conductivity $\sigma_1(\omega)$ of $\text{Sr}_3(\text{Ru}_{0.985}\text{Fe}_{0.015})_2\text{O}_7$ at several temperatures below 50 K. The blue circle indicates the energy region of the peak-like feature which appears below 35 K. The red arrow denotes the phonons. (b) The temperature dependence of the plasma frequency ω_p^2 and scattering rate $1/\tau$.

165 two different temperatures below and above 30 K, e.g. $W_S(10$
 166 $\text{K})/W_S(50\text{ K})$. The ratio is less than 1 at lower energy due to
 167 the opening of a PG in the $\sigma_1(\omega)$ spectrum at 10 K. Eventu-
 168 ally, the SW is nearly recovered and the ratio approaches 1 at
 169 much higher energies. We also calculate the W_S in three differ-
 170 ent energy intervals: $40\text{-}280\text{ cm}^{-1}$, $280\text{-}20000\text{ cm}^{-1}$, 40-
 171 20000 cm^{-1} . The temperature dependence of the normalized
 172 SW, $W_S(T)/W_S(300\text{ K})$ is displayed in Fig. 5(c), Fig. 5(d)
 173 and Fig. 5(e), respectively. It can be found that the over-
 174 all spectral weight between 40 and 20000 cm^{-1} is tempera-
 175 ture independent, and above 30 K, the SW transfer from the
 176 $280\text{-}20000\text{ cm}^{-1}$ to $40\text{-}280\text{ cm}^{-1}$ region upon cooling, which
 177 is induced by the Drude components narrowing. Below the
 178 resistivity-upturn temperature, the SW transfer from $40\text{-}280$
 179 cm^{-1} to $280\text{-}20000\text{ cm}^{-1}$ region, further confirm the formation
 180 of a PG.

181 In order to elucidate the change in electrodynamic res-
 182 sponding to the PG opening, we analyse the coherent peak
 183 quantitatively. First of all, the plasma frequency ω_p is esti-

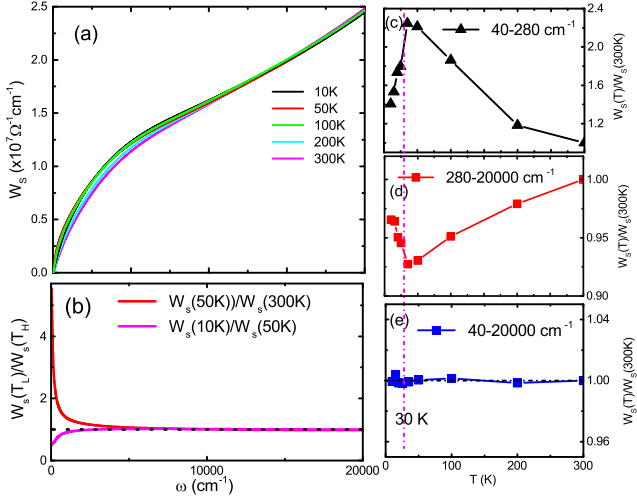


FIG. 5. (a) Upper cut off frequency dependent SW at several representative temperatures of $\text{Sr}_3(\text{Ru}_{0.985}\text{Fe}_{0.015})_2\text{O}_7$. (b) The frequency dependent of $W_S(T_L)/W_S(T_H)$. (c), (d), (e) The temperature dependence of $W_S(T)/W_S(300 \text{ K})$ between different lower and upper cutoff frequencies.

184 mated by calculating the low- ω SW, $\omega_p^2 = 8 \int_0^{\omega_c} \sigma_1(\omega) d\omega$.
 185 The cutoff frequency ω_c is chosen so as to make the inte-
 186 gration cover all contributions from free carriers and exclude
 187 contributions from interband transitions. Usually, the integral
 188 goes to a frequency where $\sigma_1(\omega)$ shows a minimum value.
 189 We expect there is a balance between the Drude component
 190 tail and the onset part of interband transition. So we choose
 191 $\omega_c = 220 \text{ cm}^{-1}$. As the PG develops, ω_p^2 decreases as temper-
 192 ature decreases, as shown in Fig. 4(b). Secondly, we estimate
 193 scattering rate $1/\tau$ using the relation $1/\tau = (1/4\pi)\rho\omega_p^2$. As the
 194 PG develops, $1/\tau$ (shown in Fig. 4(b)) also decreases as tem-
 195 perature decreases. The upturn of $\rho(T)$ below 30 K (shown
 196 in Fig. 1), could be due to the fact that ω_p^2 decreases more
 197 rapidly than $1/\tau$. Similar phenomena have been observed in
 198 $\text{Ca}_3\text{Ru}_2\text{O}_7$, 4H and 9R BaRuO_3 compounds, which also pos-
 199 sess the PG formation [20, 21].

200 We also analyse the optical conductivity with the extended
 201 Drude model, in this approach the simple Drude model is ex-
 202 tended by making the damping term in the Drude formula
 203 complex and frequency dependent [38–40]. Here the scatter-
 204 ing rate and the effective mass is allowed to have a frequency
 205 dependence.

$$\frac{1}{\tau(\omega)} = \frac{\omega_p^2}{4\pi} \frac{\sigma_1(\omega)}{\sigma_1^2(\omega) + \sigma_2^2(\omega)}. \quad (1)$$

$$\frac{m^*}{m_B} = \frac{\omega_p^2}{4\pi\omega} \frac{\sigma_2(\omega)}{\sigma_1^2(\omega) + \sigma_2^2(\omega)}. \quad (2)$$

206 where m_B is the band mass, ω_p is the plasma frequency esti-
 207 mated by calculating the low- ω SW at corresponding temper-
 208 atures as mentioned above, shown as Fig. 4(b). The obtained

209 spectra of the scattering rate and the effective mass are dis-
 210 played in Fig. 6. For clarity, only several representative tem-
 211 peratures are shown: room temperature, just above and below
 212 resistivity-upturn temperature.

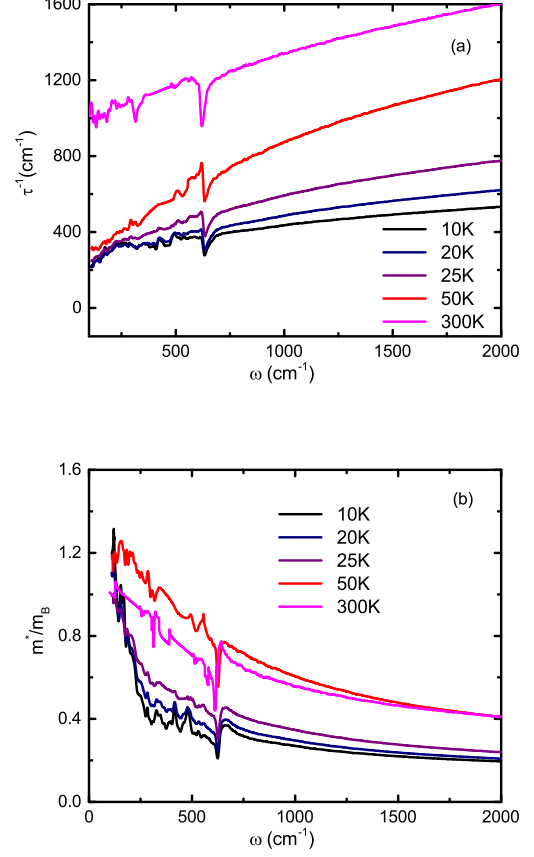


FIG. 6. Temperature dependent (a) scattering rate $1/\tau(\omega)$ and (b) effective mass m^*/m_B derived from the extended Drude model analysis.

213 Both the scattering rate and the effective mass show a pro-
 214 nounced temperature dependence at low frequencies. Notably,
 215 the scattering rate is suppressed below about 300 cm^{-1} ,
 216 and correspondingly, the effective mass is strongly enhanced.
 217 Those spectral features can also be taken as the optical signa-
 218 ture of the PG state, like the cases in cuprates [38–40], and
 219 some DW materials, $2H\text{-TaS}_2$, Na_xTaS_2 [41] and $2H\text{-NbSe}_2$
 220 [42].

221 Besides, one phonon peak at about 600 cm^{-1} is distin-
 222 guished in $\sigma_1(\omega)$ at all temperatures, as shown in Fig. 7(a),
 223 which can not be fit well by the Lorentz model, because of
 224 its asymmetric line shape. We extract the phonon line shape
 225 by subtracting a linear electronic background in a narrow fre-
 226 quency range at all measured temperatures. It is instructive to

277 fit the phonon line shape with the Fano model [43–48]:

$$\sigma_1(\omega) = \frac{2\pi}{Z_0} \frac{\Omega^2}{\gamma} \frac{q^2 + \frac{4q(\omega-\omega_0)}{\gamma} - 1}{q^2(1 + \frac{4(\omega-\omega_0)^2}{\gamma^2})}, \quad (3)$$

278 where Z_0 is the vacuum impedance; ω_0 , γ and Ω correspond to
 279 the phonon frequency, linewidth and strength of the phonon,
 280 respectively. The asymmetric phonon line shape is known
 281 to be related to electron-phonon coupling [44–46, 49, 50],
 282 and is typically characterized through the Fano- Breit-Wigner
 283 (FBW) parameter q . The physical meaning of q is that it is
 284 inversely related to the strength of the electron-phonon coupling.
 285 Therefore, a larger $1/q^2$ (the Fano factor) indicates
 286 more conspicuous asymmetry in the phonon line shape, while
 287 for $1/q^2 = 0$, the symmetric Lorentz line shape is fully re-
 288 covered. The Fano factors $1/q^2$, determined from the fittings,
 289 are shown in Fig. 7(b). We found that above 30 K, $1/q^2$ in-
 290 creases slightly with temperature decreasing; however, below
 291 30 K, it increases significantly, reflecting enhancement of the
 292 electron-phonon coupling.

293 The linewidth γ of the Fano resonance (shown as the black
 294 line in Fig. 7(c)) decreases continuously until 30 K, below
 295 which temperature, γ shows a clear upturn. For the electron-
 296 phonon interaction process, the phonon linewidth γ is indica-
 297 tive of the related electron-phonon coupling strength. How-
 298 ever, the phonon linewidth is related to two processes: $\gamma(T) =$
 299 $\gamma^{ph-ph}(T) + \gamma^{e-ph}(T)$, where $\gamma^{e-ph}(T)$ and $\gamma^{ph-ph}(T)$ represent
 300 the electron-phonon (e-ph) and anharmonic phonon-phonon
 301 (ph-ph) interactions. The e-ph (ph-ph) interaction gives an in-
 302 creasing (decreasing) linewidth as the temperature is reduced.
 303 Thus the temperature dependence of the total γ is a balance of
 304 $\gamma^{e-ph}(T)$ and $\gamma^{ph-ph}(T)$ [51]. At temperature above 30 K, the
 305 electron-phonon coupling is weak, in this case, phonon decay
 306 is dominated by the anharmonic effect: a zone-centre phonon
 307 decays into two acoustic modes with the same frequencies and
 308 opposite momenta [52, 53], so $\gamma^{ph-ph}(T)$ dominates. The tem-
 309 perature dependence of the phonon linewidth $\gamma^{ph-ph}(T)$ for
 310 this process follows $\gamma^{ph-ph}(T) = \gamma_0^{ph-ph}(1 + \frac{2}{e^{\frac{\hbar\omega_0}{2k_B T}} - 1})$, where
 311 γ_0^{ph-ph} is the residual linewidth at zero temperature. Appar-
 312 ently, this model can account for the decreasing γ as the tem-
 313 perature is decreased. At temperature below 30 K, the up-
 314 turn of γ might be arise from strong electron-phonon coupling
 315 mechanism. If the electron-phonon coupling is strong, a phonon
 316 can also decay by creating an electron-hole pair [54], resulting
 317 in a temperature-dependent phonon linewidth $\gamma^{e-ph}(T)$, $\gamma^{e-ph}(T) =$
 318 $\gamma_0^{e-ph} D_{e-h}(\omega_0, T)$, where $D_{e-h}(\omega_0, T)$ is the finite-temper-
 319 ature joint electron-hole pair density of states at $\hbar\omega_0$ (the energy
 320 of the phonon peak).

321 As mentioned above, we propose that a PG opens below the
 322 resistivity-upturn temperature. This results in a suppressed
 323 SW at lower frequency transfers to a peak-like feature with
 324 its central frequency at about 350 cm^{-1} (shown as the blue
 325 circle in Fig. 3(a)). Thus, this brings up the possibility of
 326 changes to the electronic states in this system. That is, the
 327 electronic density of states (DOS) increase obviously at the

278 peak-like feature energy region, which could contribute to the
 279 increasing γ below 30 K, and results in a significant increase
 280 of the electron-phonon coupling. Thus the line shape of the
 281 phonon peaks become more asymmetric, leading to a signif-
 282 icant increase of $1/q^2$. Therefore, the significant increase of
 283 $1/q^2$ and γ in present study can be attributed to the formation
 284 of the peak-like structure around 350 cm^{-1} . Thus the tem-
 285 perature evolution of $1/q^2$ and γ gives further evidence for
 286 the opening of a PG accompanied with the resistivity-upturn
 287 behavior. Similar enhancement of Fano factor was also re-
 288 ported in CaFeO_3 [50], and was attributed to the changing of
 289 the electron-phonon coupling and the electronic DOS due to
 290 a gap opening feature below a charge-disproportionation tran-
 291 sition temperature. In addition, we show the temperature de-
 292 pendence of the phonon frequency (ω_0) in Fig. 7(d). It cor-
 293 responds to the peak frequency of the in-plane Ru-O stretching
 294 mode [55, 56]; and exhibits the usual hardening for decreasing
 295 temperature, due to the crystal contraction.

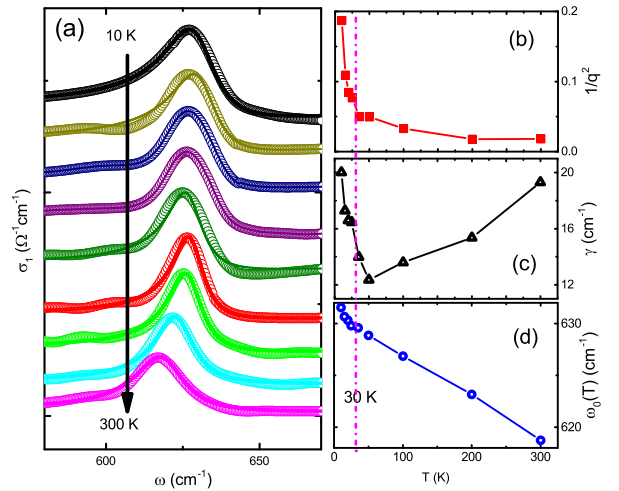


FIG. 7. (a) Line shape of the infrared phonon modes in $\text{Sr}_3(\text{Ru}_{0.985}\text{Fe}_{0.015})_2\text{O}_7$. The solid lines through the data denote the Fano fitting results. Temperature dependence of (b) the Fano factor $1/q^2$, (c) the linewidth γ , (d) the frequency of the phonons. The solid lines are guide to the eye.

329 It is remarkable that $\text{Sr}_3(\text{Ru}_{0.985}\text{Fe}_{0.015})_2\text{O}_7$ shows PG phe-
 330 nomena coherently in transport and optical properties. To un-
 331 derstand the origin of the PG in $\text{Sr}_3(\text{Ru}_{0.985}\text{Fe}_{0.015})_2\text{O}_7$, there
 332 are several experimental facts which should be taken into ac-
 333 count. First of all, the dip in $R(\omega)$ and corresponding peak-
 334 like feature in $\sigma_1(\omega)$ may remind of DW materials. As for
 335 a DW order, the opening of an energy gap leads to a SW
 336 suppression below 2Δ (the energy gap) and a nonsymmetric
 337 peak with clear edge-like feature near 2Δ in the optical con-
 338 ductivity. Secondly, the observed PG features are similar to
 339 four-layer, nine-layer BaRuO_3 compounds [20, 21], and its
 isostructural compound $\text{Ca}_3\text{Ru}_2\text{O}_7$ [29], where they ascribed
 the PG to the partial gap opening due to the DW instability.
 Thirdly, for $\text{Sr}_3\text{Ru}_2\text{O}_7$, due to its strong magnetic fluctuations,

a magnetic field and magnetic impurities can profoundly affect the magnetic and electronic properties. The magnetic neutron scattering study of $\text{Sr}_3\text{Ru}_2\text{O}_7$ shows that the application of a magnetic field can tune it through two magnetically ordered spin density wave (SDW) states [57]. Hence the doping of magnetic impurities (Fe) may act as the role of a magnetic field with the possibility to induce SDW order. Further study is required regarding the formation of a DW order in $\text{Sr}_3(\text{Ru}_{0.985}\text{Fe}_{0.015})_2\text{O}_7$. Nevertheless, the dip in $R(\omega)$ and corresponding peak-like feature in $\sigma_1(\omega)$, accompanied by the enhancement of $1/q^2$ and γ below the resistivity-upturn temperature are sufficient enough to indicate that there is a PG opening behavior.

CONCLUSION

In summary, an upturn of the resistivity is observed in $\text{Sr}_3(\text{Ru}_{0.985}\text{Fe}_{0.015})_2\text{O}_7$ at about 30 K. Optical spectroscopy

study find a clear dip in $R(\omega)$ which corresponds to a peak-like feature in $\sigma_1(\omega)$ and a suppression in scattering rate $1/\tau(\omega)$, indicating the formation of a PG accompanied with the resistivity-upturn behavior. Moreover, the significant increase of Fano factor $1/q^2$ and linewidth γ below this temperature gives further evidence for the opening of a PG, which might originate from the partial k-space gap opening due to DW instability.

ACKNOWLEDGMENTS The authors acknowledge the support of NSAF, Grant No. U1530402. The work (single crystal growth and characterization) at Tulane is supported by the US Department of Energy (DOE) under EPSCoR Grant No. DE-SC0012432 with additional support from the Louisiana Board of Regents.

* hong.xiao@hpstar.ac.cn

- [1] Y. Yoshida, I. Nagai, S.-I. Ikeda, N. Shirakawa, M. Kosaka, and N. Môri, *Phys. Rev. B* **69**, 220411 (2004).
- [2] N. Kikugawa, A. W. Rost, C. W. Hicks, A. J. Schofield, and A. P. Mackenzie, *Journal of the Physical Society of Japan* **79**, 024704 (2010).
- [3] A. P. Mackenzie and Y. Maeno, *Rev. Mod. Phys.* **75**, 657 (2003).
- [4] Y. Maeno, S. Kittaka, T. Nomura, S. Yonezawa, and K. Ishida, *Journal of the Physical Society of Japan* **81**, 011009 (2012).
- [5] S. Nakatsuji and Y. Maeno, *Phys. Rev. Lett.* **84**, 2666 (2000).
- [6] G. Cao, S. McCall, J. E. Crow, and R. P. Guertin, *Phys. Rev. Lett.* **78**, 1751 (1997).
- [7] W. Bao, Z. Q. Mao, Z. Qu, and J. W. Lynn, *Phys. Rev. Lett.* **100**, 247203 (2008).
- [8] S.-I. Ikeda, Y. Maeno, S. Nakatsuji, M. Kosaka, and Y. Uwatoko, *Phys. Rev. B* **62**, R6089 (2000).
- [9] S. A. Grigera, R. S. Perry, A. J. Schofield, M. Chiao, S. R. Julian, G. G. Lonzarich, S. I. Ikeda, Y. Maeno, A. J. Millis, and A. P. Mackenzie, *Science* **294**, 329 (2001).
- [10] R. A. Borzi, S. A. Grigera, J. Farrell, R. S. Perry, S. J. S. Lister, S. L. Lee, D. A. Tennant, Y. Maeno, and A. P. Mackenzie, *Science* **315**, 214 (2007).
- [11] L. Capogna, E. M. Forgan, S. M. Hayden, A. Wildes, J. A. Duffy, A. P. Mackenzie, R. S. Perry, S. Ikeda, Y. Maeno, and S. P. Brown, *Phys. Rev. B* **67**, 012504 (2003).
- [12] K. Kitagawa, K. Ishida, R. S. Perry, T. Tayama, T. Sakakibara, and Y. Maeno, *Phys. Rev. Lett.* **95**, 127001 (2005).
- [13] E. Dagotto, *Science* **309**, 257 (2005).
- [14] Z. Fang and K. Terakura, *Phys. Rev. B* **64**, 020509 (2001).
- [15] M. Zhu, Y. Wang, P. G. Li, J. J. Ge, W. Tian, D. Keavney, Z. Q. Mao, and X. Ke, *Phys. Rev. B* **95**, 174430 (2017).
- [16] C. Mirri, F. M. Vitucci, P. Di Pietro, S. Lupi, R. Fittipaldi, V. Granata, A. Vecchione, U. Schade, and P. Calvani, *Phys. Rev. B* **85**, 235124 (2012).
- [17] P. Steffens, J. Farrell, S. Price, A. P. Mackenzie, Y. Sidis, K. Schmalzl, and M. Braden, *Phys. Rev. B* **79**, 054422 (2009).
- [18] R. Mathieu, A. Asamitsu, Y. Kaneko, J. P. He, X. Z. Yu, R. Kumai, Y. Onose, N. Takeshita, T. Arima, H. Takagi, and Y. Tokura, *Phys. Rev. B* **72**, 092404 (2005).
- [19] M. A. Hossain, B. Bohnenbuck, Y. D. Chuang, M. W. Haverkort, I. S. Elfimov, A. Tanaka, A. G. Cruz Gonzalez, Z. Hu, H.-J. Lin, C. T. Chen, R. Mathieu, Y. Tokura, Y. Yoshida, L. H. Tjeng, Z. Hussain, B. Keimer, G. A. Sawatzky, and A. Damascelli, *Phys. Rev. B* **86**, 041102 (2012).
- [20] Y. S. Lee, J. S. Lee, K. W. Kim, T. W. Noh, J. Yu, Y. Bang, M. K. Lee, and C. B. Eom, *Phys. Rev. B* **64**, 165109 (2001).
- [21] Y. S. Lee, J. S. Lee, K. W. Kim, T. W. Noh, J. Yu, E. J. Choi, G. Cao, and J. E. Crow, *EPL (Europhysics Letters)* **55**, 280 (2001).
- [22] K. Pucher, A. Loidl, N. Kikugawa, and Y. Maeno, *Phys. Rev. B* **68**, 214502 (2003).
- [23] H. Ding, T. Yokoya, J. C. Campuzano, T. Takahashi, M. Randeria, M. R. Norman, T. Mochiku, K. Kadowaki, and J. Giapintzakis, *Nature* **382**, 51 (1996).
- [24] M. R. Norman, H. Ding, M. Randeria, J. C. Campuzano, T. Yokoya, T. Takeuchi, T. Takahashi, T. Mochiku, K. Kadowaki, P. Guptasarma, and D. G. Hinks, *Nature* **392**, 157 (1998).
- [25] C. Renner, B. Revaz, J.-Y. Genoud, K. Kadowaki, and O. Fischer, *Phys. Rev. Lett.* **80**, 149 (1998).
- [26] Y. M. Dai, B. Xu, P. Cheng, H. Q. Luo, H. H. Wen, X. G. Qiu, and R. P. S. M. Lobo, *Phys. Rev. B* **85**, 092504 (2012).
- [27] T. Dong, F. Zhou, and N. L. Wang, *Phys. Rev. B* **88**, 184507 (2013).
- [28] S. J. Moon, Y. S. Lee, A. A. Schafgans, A. V. Chubukov, S. Kasahara, T. Shibauchi, T. Terashima, Y. Matsuda, M. A. Tanatar, R. Prozorov,

- 377 A. Thaler, P. C. Canfield, S. L. Bud'ko, A. S. Sefat, D. Mandrus, K. Segawa, Y. Ando, and D. N. Basov, *Phys. Rev. B* **90**, 014503 (2014).
- 378 [29] J. S. Lee, S. J. Moon, B. J. Yang, J. Yu, U. Schade, Y. Yoshida, S.-I. Ikeda, and T. W. Noh, *Phys. Rev. Lett.* **98**, 097403 (2007).
- 379 [30] M. Imada, A. Fujimori, and Y. Tokura, *Rev. Mod. Phys.* **70**, 1039 (1998).
- 380 [31] D. J. Singh and I. I. Mazin, *Phys. Rev. B* **63**, 165101 (2001).
- 381 [32] M. B. Stone, M. D. Lumsden, R. Jin, B. C. Sales, D. Mandrus, S. E. Nagler, and Y. Qiu, *Phys. Rev. B* **73**, 174426 (2006).
- 382 [33] S. Ramos, E. Forgan, C. Bowell, S. Hayden, A. Schofield, A. Wildes, E. Yelland, S. Brown, M. Laver, R. Perry, and Y. Maeno, *Physica B: Condensed Matter* **403**, 1270 (2008).
- 383 [34] D. Mesa, F. Ye, S. Chi, J. A. Fernandez-Baca, W. Tian, B. Hu, R. Jin, E. W. Plummer, and J. Zhang, *Phys. Rev. B* **85**, 180410 (2012).
- 384 [35] B. Hu, G. T. McCandless, V. O. Garlea, S. Stadler, Y. Xiong, J. Y. Chan, E. W. Plummer, and R. Jin, *Phys. Rev. B* **84**, 174411 (2011).
- 385 [36] C. C. Homes, M. Reedyk, D. A. Cradles, and T. Timusk, *Appl. Opt.* **32**, 2976 (1993).
- 386 [37] D. B. Tanner, *Phys. Rev. B* **91**, 035123 (2015).
- 387 [38] D. N. Basov and T. Timusk, *Rev. Mod. Phys.* **77**, 721 (2005).
- 388 [39] P. B. Allen, *Phys. Rev. B* **3**, 305 (1971).
- 389 [40] A. V. Puchkov, D. N. Basov, and T. Timusk, *Journal of Physics: Condensed Matter* **8**, 10049 (1996).
- 390 [41] W. Z. Hu, G. Li, J. Yan, H. H. Wen, G. Wu, X. H. Chen, and N. L. Wang, *Phys. Rev. B* **76**, 045103 (2007).
- 391 [42] S. V. Dordevic, D. N. Basov, R. C. Dynes, and E. Bucher, *Phys. Rev. B* **64**, 161103 (2001).
- 392 [43] R. Yang, Y. Dai, B. Xu, W. Zhang, Z. Qiu, Q. Sui, C. C. Homes, and X. Qiu, *Phys. Rev. B* **95**, 064506 (2017).
- 393 [44] B. Xu, Y. Dai, J. Han, K. Wang, R. Yang, Y. Yang, W. Zhang, H. Xiao, and X. Qiu, *Physica C: Superconductivity and its Applications* **503**, 25 (2014).
- 394 [45] W. J. Padilla, M. Dumm, S. Komiya, Y. Ando, and D. N. Basov, *Phys. Rev. B* **72**, 205101 (2005).
- 395 [46] A. B. Kuzmenko, L. Benfatto, E. Cappelluti, I. Crassee, D. van der Marel, P. Blake, K. S. Novoselov, and A. K. Geim, *Phys. Rev. Lett.* **103**, 116804 (2009).
- 396 [47] B. Xu, Y. M. Dai, B. Shen, H. Xiao, Z. R. Ye, A. Forget, D. Colson, D. L. Feng, H. H. Wen, C. C. Homes, X. G. Qiu, and R. P. S. M. Lobo, *Phys. Rev. B* **91**, 104510 (2015).
- 397 [48] B. Xu, H. Xiao, B. Gao, Y. H. Ma, G. Mu, P. Marsik, E. Sheveleva, F. Lyzwa, Y. M. Dai, R. P. S. M. Lobo, and C. Bernhard, *Phys. Rev. B* **97**, 195110 (2018).
- 398 [49] K.-Y. Choi, Y. G. Pashkevich, K. V. Lamonova, H. Kageyama, Y. Ueda, and P. Lemmens, *Phys. Rev. B* **68**, 104418 (2003).
- 399 [50] C. X. Zhang, H. L. Xia, H. Liu, Y. M. Dai, B. Xu, R. Yang, Z. Y. Qiu, Q. T. Sui, Y. W. Long, S. Meng, and X. G. Qiu, *Phys. Rev. B* **95**, 064104 (2017).
- 400 [51] B. Xu, Y. Dai, L. Zhao, K. Wang, R. Yang, W. Zhang, J. Liu, H. Xiao, G. Chen, S. Trugman, J.-X. Zhu, A. Taylor, D. Yarotski, R. Prasankumar, and X. Qiu, *Nature communications* **8**, 14933 (2017).
- 401 [52] P. G. Klemens, *Phys. Rev.* **148**, 845 (1966).
- 402 [53] J. Menéndez and M. Cardona, *Phys. Rev. B* **29**, 2051 (1984).
- 403 [54] N. Bonini, M. Lazzeri, N. Marzari, and F. Mauri, *Phys. Rev. Lett.* **99**, 176802 (2007).
- 404 [55] C. Mirri, L. Baldassarre, S. Lupi, M. Ortolani, R. Fittipaldi, A. Vecchione, and P. Calvani, *Phys. Rev. B* **78**, 155132 (2008).
- 405 [56] J. S. Lee, Y. S. Lee, T. W. Noh, S. Nakatsuji, H. Fukazawa, R. S. Perry, Y. Maeno, Y. Yoshida, S. I. Ikeda, J. Yu, and C. B. Eom, *Phys. Rev. B* **70**, 085103 (2004).
- 406 [57] C. Lester, S. Ramos, R. S. Perry, T. P. Croft, R. I. Bewley, T. Guidi, P. Manuel, D. D. Khalyavin, E. M. Forgan, and S. M. Hayden, *nature materials* **10.1038/nmat4181**.
- 407
- 408
- 409
- 410
- 411
- 412
- 413
- 414
- 415